Analysis of high-temperature performance of 4H-SiC avalanche photodiodes in both linear and Geiger modes

Xing-Ye Zhou(周幸叶), Yuan-Jie Lv(吕元杰)[†], Hong-Yu Guo(郭红雨), Guo-Dong Gu(顾国栋), Yuan-Gang Wang(王元刚), Shi-Xiong Liang(梁士雄), Ai-Min Bu(卜爱民), and Zhi-Hong Feng(冯志红)[‡]

National Key Laboratory of ASIC, Hebei Semiconductor Research Institute, Shijiazhuang 050051, *China*

(Received 21 June 2022; revised manuscript received 1 October 2022; accepted manuscript online 7 October 2022)

The high-temperature performance of 4H-SiC ultraviolet avalanche photodiodes (APDs) in both linear and Geiger modes is extensively investigated. During the temperature-dependent measurements, a fixed bias voltage is adopted for the device samples, which is much more practical and important for high-temperature applications. The results show that the fabricated 4H-SiC APDs are very stable and reliable at high temperatures. As the temperature increases from room temperature to 425 K, the dark current at 95% of the breakdown voltage increases slightly and remains lower than 40 pA. In Geiger mode, our 4H-SiC APDs can be self-quenched in a passive-quenching circuit, which is expected for high-speed detection systems. Moreover, an interesting phenomenon is observed for the first time: the single-photon detection efficiency shows a non-monotonic variation as a function of temperature. The physical mechanism of the variation in high-temperature performance is further analyzed. The results in this work can provide a fundamental reference for researchers in the field of 4H-SiC APD ultraviolet detectors.

Keywords: 4H-SiC, avalanche photodiode, ultraviolet detector, high temperature

PACS: 85.60.Gz, 85.60.Dw, 85.60.Bt, 95.85.Mt **DOI:** 10.1088/1674-1056/ac9820

1. Introduction

With its advantages of low dark current, high quantum efficiency, high reliability and easy integration, a wide-bandgap semiconductor 4H-SiC avalanche photodiode (APD) is a potential ultraviolet (UV) detector to replace photomultiplier tubes (PMTs) in applications such as flame detection, corona detection, UV communication, astronomical research, missile plume detection, etc.[1–16] Great improvements have been made to 4H-SiC APDs and related arrays during the past two decades.[17–23] Benefiting from the wide bandgap and high thermal conductivity of 4H-SiC material, 4H-SiC APDs are expected to be very stable and reliable as the temperature varies. Dependence of the performance of 4H-SiC APDs on temperature has been investigated by some research groups.[24–27] The single-photon detection performance at high temperatures[26] and dark count mechanisms at low temperatures[27] have been studied. However, the previously reported research work on the temperature-dependent performance of 4H-SiC APDs was based on a fixed optical gain or fixed single-photon detection efficiency (SPDE). This means that the bias voltage of 4H-SiC APDs must be adjusted at different temperatures during the measurement process to maintain the gain or SPDE constant obtained in Refs. [26,27], which is not practical. So far, the impact of temperature on the device performance of 4H-SiC APDs at a fixed bias voltage has not been investigated; this would be more useful and important for practical applications.

In this work, the high-temperature performance of 4H-SiC APDs is extensively investigated in both linear and Geiger modes. A fixed bias voltage was adopted for devices during characterization and measurements at various temperatures. The results demonstrate that the fabricated 4H-SiC APDs are very stable and reliable at high temperatures even in an air atmosphere. As the temperature increases from room temperature to 425 K, the dark current at 95% of the breakdown voltage increases slightly and remains lower than 40 pA. In addition, the avalanche breakdown voltage shows a very small positive coefficient of < 8 mV·K^{-1}. In Geiger mode, the dark count rate (DCR) increases with increasing temperature, while the SPDE exhibits a non-monotonic variation as a function of temperature; this is the first time this has been observed and reported. The corresponding physical mechanisms of the high-temperature performances are further analyzed and discussed.

2. Device structure and fabrication

In this work, a separate absorption charge multiplication epilayer structure for 4H-SiC APDs was grown by chemical vapor deposition, as shown in Fig. 1(a). From bottom to top, the device structure comprises a p^+ layer with a thickness of 3 μm, an n^- multiplication layer with thickness of 0.5 μm, an n charge layer with a thickness of 0.2 μm, an n^- absorption layer with a thickness of 0.5 μm and an n^+ contact layer with a thickness of 0.3 μm. The corresponding doping concentration of the epilayers is 1×10^{19} cm^{-3}, 1×10^{15} cm^{-3},

[†]Corresponding author. E-mail: yuanjielv@163.com
[‡]Corresponding author. E-mail: ga917vv@163.com

© 2023 Chinese Physical Society and IOP Publishing Ltd

1×10^{18} cm^{-3}, 1×10^{15} cm^{-3}, and 2×10^{19} cm^{-3}, respectively.

Fabrication of the 4H-SiC APDs was based on our optimized device processing technology.[23] First, a positively beveled mesa was created based on a variable-temperature photoresist reflow technique and inductively coupled plasma (ICP) dry etching. After that, a Ni/Ti/Al/Au (35 nm/50 nm/150 nm/100 nm) metal stack was formed for anode and cathode Ohmic contacts, during which rapid thermal annealing was carried out at 800 °C for 3 min in a N_2 atmosphere. Then, a 500 nm thick SiN_x layer was deposited for passivation by dual-frequency plasma enhanced chemical vapor deposition (PECVD). After removing the SiN_x layer in the contact area by ICP etching, a Ti/Au (20 nm/200 nm) metal stack was deposited for bonding pads. Finally, the optical window was opened by removing the SiN_x layer in the active area. The diameter of the active area of the fabricated 4H-SiC APDs is 150 μm. A photograph of the device is shown in Fig. 1(b).

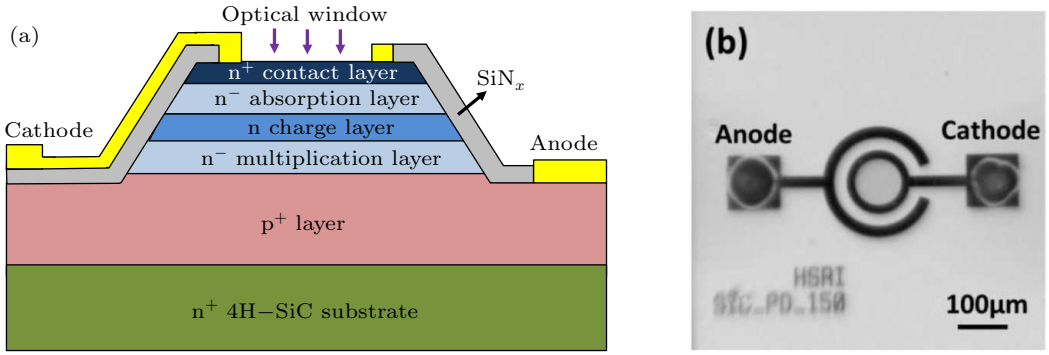


Fig. 1. Structure of the 4H-SiC APD in this work: (a) schematic cross section; (b) photograph of the fabricated device.

3. Results and discussion

In this section, the impact of temperature on the performance of 4H-SiC UV APDs is extensively investigated in both linear and Geiger modes, and the corresponding physical mechanisms are also analyzed.

First, the room-temperature characteristics of 4H-SiC APDs were investigated in both linear and Geiger modes. In the linear mode, the currents with and without UV illumination as well as the multiplication gain of 4H-SiC APDs were characterized as a function of reverse voltage, as shown in Fig. 2(a). It can be seen that a low dark current is maintained at about 10 pA before avalanche breakdown (∼ 163.5 V). A high multiplication gain of 10^6 is obtained according to $M = (I_{\text{photo}} - I_{\text{dark}})/(I_{\text{photo_unity}} - I_{\text{dark_unity}})$, where unity gain is defined at the reverse bias of $V_r = 10$ V. In addition, the responsivity of 4H-SiC APDs was measured at unity gain based on a monochromator, a xenon lamp light source and a silicon UV photodetector for calibration. As shown in the inset of Fig. 2(a), at a wavelength of 285 nm, a peak responsivity of 0.12 A·W^{-1} is obtained, corresponding to the maximum quantum efficiency of 52%.

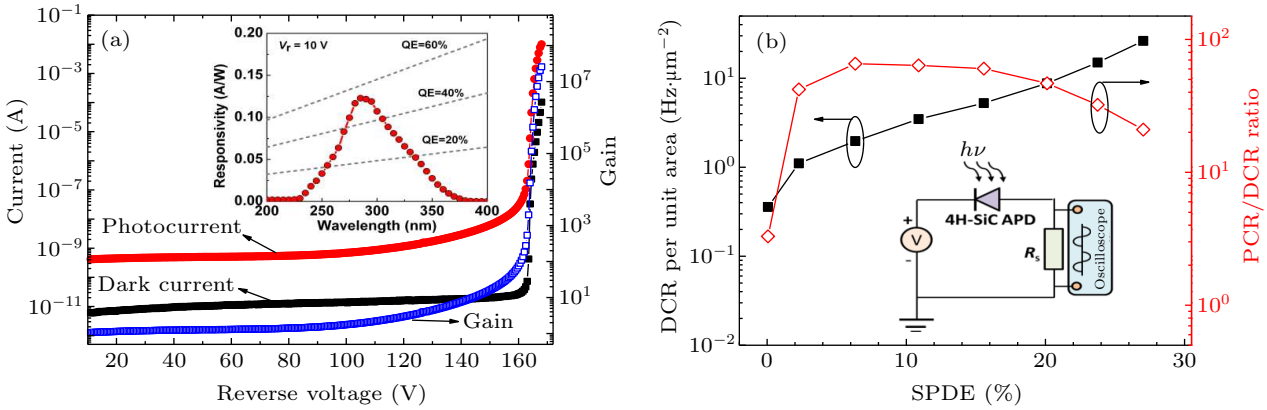


Fig. 2. Characteristics of the 4H-SiC APD at room temperature: (a) linear mode; (b) Geiger mode.

In Geiger mode, 4H-SiC APDs are able to detect extremely low-level UV signals or even a single photon. Measurement results for the single-photon detection performance of our 4H-SiC APDs are illustrated in Fig. 2(b); these were obtained by using a passive-quenching circuit (see the inset in Fig. 2(b)). It should be noted that our 4H-SiC APD can be self-quenched without a large quenching series resistor in the passive-quenching circuit, which is as expected for a high photon count rate (PCR) in high-speed detection applications. During measurement of the single-photon detection

performance, the 4H-SiC APD sample was biased above the avalanche breakdown voltage and the incident UV photon flux was attenuated to a very low level (~ 870 photons·s^{-1}·μm^{-2}). In a 4H-SiC APD biased in Geiger mode, the photon-generated carriers may experience avalanche multiplication in the high electric field, and each multiplied carrier will lead to a voltage pulse on the sampling resistor. In this work, a sampling resistor of $R_s = 500\ \Omega$ was adopted for collecting the output pulse signals, and the output pulse signals were recorded by a 2.5 GHz oscilloscope with a sampling rate of 10 GS·s^{-1}. As shown in Fig. 2(b), the dark count rate (DCR) increases with increasing SPDE, while a peak is observed in the ratio of PCR to DCR as the SPDE varies. Given a DCR of 10 Hz·μm^{-2}, a high SPDE of 20% is achieved for our devices. Meanwhile, a signal to noise ratio (PCR/DCR ratio) of more than 45 is also obtained. The results show that the fabricated 4H-SiC APDs have an excellent performance in both linear and Geiger modes at room temperature.

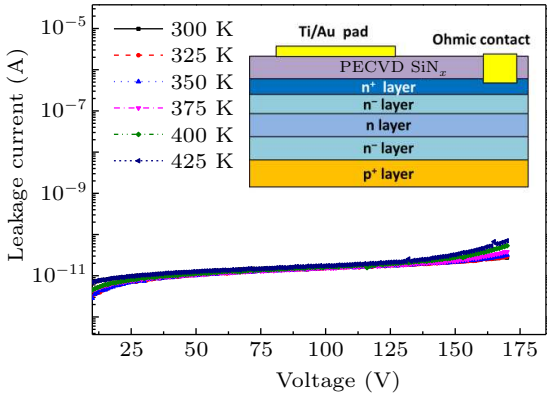


Fig. 3. Temperature-dependent measurement results for leakage current of the test structure with a dual-frequency PECVD SiN_x passivation layer; the test structure is shown in the inset.

Dark current is one of the key parameters for APD devices, and is expected to be as low as possible. SiO_2 passivation is usually used to suppress the surface leakage current for SiC APDs. However, PECVD SiO_2 film is not good enough to control the surface leakage. A thermally grown SiO_2 layer is thin and time-consuming to grow, although the film quality is better than PECVD SiO_2. Additionally, SiO_2 passivation is prone to degradation in harsh environments. Due to its chemical stability, SiN_x can enable devices to operate in harsh environments. In order to check the suppression of leakage current by a SiN_x passivation layer at high temperatures, a test structure was additionally designed and fabricated in this work on the same template, which has an Ohmic contact on the epilayer surface and a Ti/Au pad on the passivation layer, as shown in the inset of Fig. 3. It can be seen from Fig. 3 that there is no obvious change in the surface leakage current of the test structure measured at various temperatures from 300 K to 425 K. In addition, the leakage currents are lower than 100 pA even at 170 V, which proves that the dual-frequency PECVD SiN_x passivation layer can effectively reduce the surface leakage current at high reverse voltages and high temperatures.

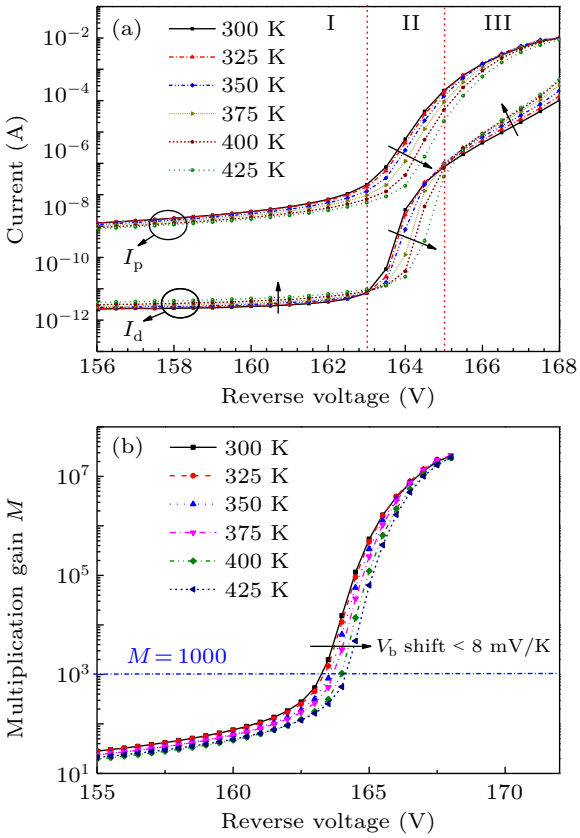


Fig. 4. Performances of 4H-SiC APDs in linear mode at different temperatures: (a) *I*–*V* curves; (b) *M*–*V* curves.

As plotted in Fig. 4(a), the *I*–*V* characteristics of our 4H-SiC APDs with and without UV illumination were measured at different temperatures to investigate the high-temperature device performance. As seen from Fig. 4(a), just a very slight variation is observed for the dark and photocurrents as the temperature changes from 300 K to 425 K, indicating high-temperature stability for our 4H-SiC APD devices. It is interesting that the reverse *I*–*V* curves with different temperatures can be divided into three regions (I, II, and III), and the temperature-dependent variation trends of the reverse current are different in the three regions. In region I, the reverse voltage is very low, and consequently the electric field is not strong. As the temperature increases, the small increase in the dark current mainly results from thermally generated carriers. In region II, with increasing temperature the dark current decreases due to the reduced impact ionization coefficient,[28] leading to a positive shift in avalanche breakdown voltage. This suggests that hard avalanche breakdown occurs in our devices, which is expected for high-gain APDs. In region III, the dark current is positively dependent on the temperature again, which is related to the parasitic series resistance in 4H-SiC APDs. The self-quenching capability of our 4H-SiC APDs may be explained by the parasitic series resistance which can act as a quenching resistor in Geiger mode. In

Fig. 4(b), the multiplication gain at various temperatures is plotted as a function of reverse voltage near the breakdown voltage (V_b). It is shown that the avalanche breakdown voltage shifts with a small temperature coefficient of < 8 mV·K^{-1}, where the breakdown voltage is defined as the reverse voltage with a multiplication gain of 1000.

The dark current at 95% of breakdown voltage is extracted as a function of temperature, as shown in Fig. 5(a). The dark current of 4H-SiC APDs before the breakdown voltage increases slightly with increasing temperature, which results from the increased number of electron–hole pairs generated in the semiconductor at high temperatures. Benefiting from the wide bandgap and high thermal conductivity of 4H-SiC, the dark current at 95% of V_b remains lower than 40 pA for our APDs, even at 425 K (see Fig. 5(a)). The multiplication gain as a function of temperature is shown in Fig. 5(b). Since the impact ionization coefficient decreases with increasing temperature, the multiplication gain will consequently decline as the temperature rises. It can be seen from Fig. 5(b) that the multiplication gain stays at over 10^6 as the temperature increases from 300 K to 425 K.

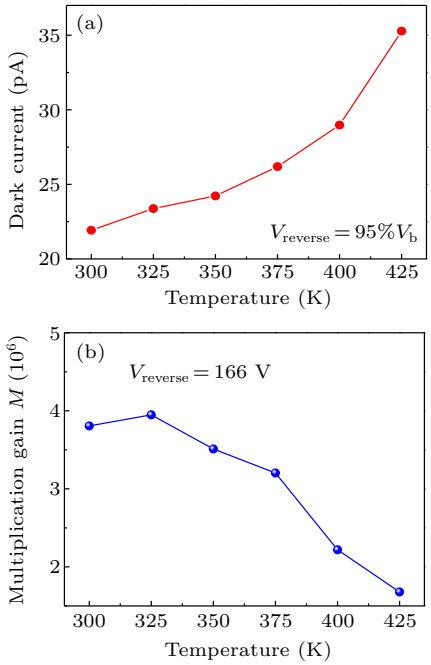


Fig. 5. Dark current and multiplication gain as a function of temperature for 4H-SiC APDs.

Based on a simple passive quenching circuit (see the inset in Fig. 2(b)), the single-photon counting measurements in Geiger mode were conducted at various temperatures in this work. The dark count and photon count spectra of our 4H-SiC APDs with a reverse bias voltage of 166 V at temperatures of 300 K, 350 K, and 425 K are also shown in Fig. 6. Since the noise floor of the measurement system is ~ 2 mV, a threshold voltage of $V_{th} = 15$ mV is chosen to discriminate the output signals from the background noise. We can see that the output pulse height is of the order of tens of mV, which is far higher than the noise floor (~ 2 mV). With a threshold voltage of $V_{th} = 15$ mV, the output pulses over 15 mV are all counted for the measurement of single-photon detection. It is very clear that the DCR keeps increasing as the temperature changes from 300 K to 425 K, while PCR rises first and then declines.

In order to show the variation of DCR and SPDE more clearly and obviously, the dependence of DCR and SPDE on the temperature is shown in Fig. 7 for 4H-SiC APDs at different bias voltages. Figures 7(a)–7(c) provide the DCR and SPDE as a function of temperature at 166 V, 167 V, and 168 V, respectively. At a fixed temperature, both DCR and SPDE increase as the bias voltage increases. For example, with the bias voltage increasing from 166 V to 168 V at a temperature of 375 K, DCR increases from 7.1 Hz·μm^{-2} to 100 Hz·μm^{-2} and the SPDE increases from 11.57% to 42.66%, respectively, which is consistent with the results in Fig. 6. Moreover, it is shown that the dark count rate is positively dependent on the temperature, which is consistent with the dark current and can be explained by the thermally generated carriers. The higher the temperature, the greater the number of thermally generated carriers, causing an increased dark count rate. However, the SPDE in this work shows a non-monotonic variation as a function of temperature, which is different from the results in Ref. [26]. The SPDE of 4H-SiC APDs declined monotonically with increasing temperature in Ref. [26], where the SPDE actually corresponded to different bias voltages since the bias voltage had to be adjusted at different temperatures to keep the gain of the device constant. In this work, a fixed voltage is maintained. For the first time, an interesting phenomenon is observed, namely there is a peak in the SPDE curve as a function of temperature from 300 K to 425 K, as shown in Figs. 7(a)–7(c), where the trends in temperature-dependent variation of SPDE at bias voltages of 166 V, 167 V, and 168 V are similar.

The mechanism of SPDE variation observed in this work may be explained as follows. Since the total number of incident UV photons is constant during the measurement, the variation of SPDE is correlated to the change in PCR. That is to say, at a given bias voltage (e.g., 166 V), PCR first increases then decreases with increasing temperature. This is a combined result of the temperature-dependent responsivity and impact ionization coefficient. It has been proved that the responsivity is positively dependent on temperature,[24–26] while the impact ionization coefficient decreases with increasing temperature.[28] As the temperature increases from 300 K, increased responsivity of 4H-SiC APDs leads to more photon-generated carriers and higher PCR. However, as the temperature increases further, the impact ionization coefficient will be a dominant factor in the decrease in PCR. That is why SPDE varies nonmonotonically with increasing temperature at a fixed bias voltage.

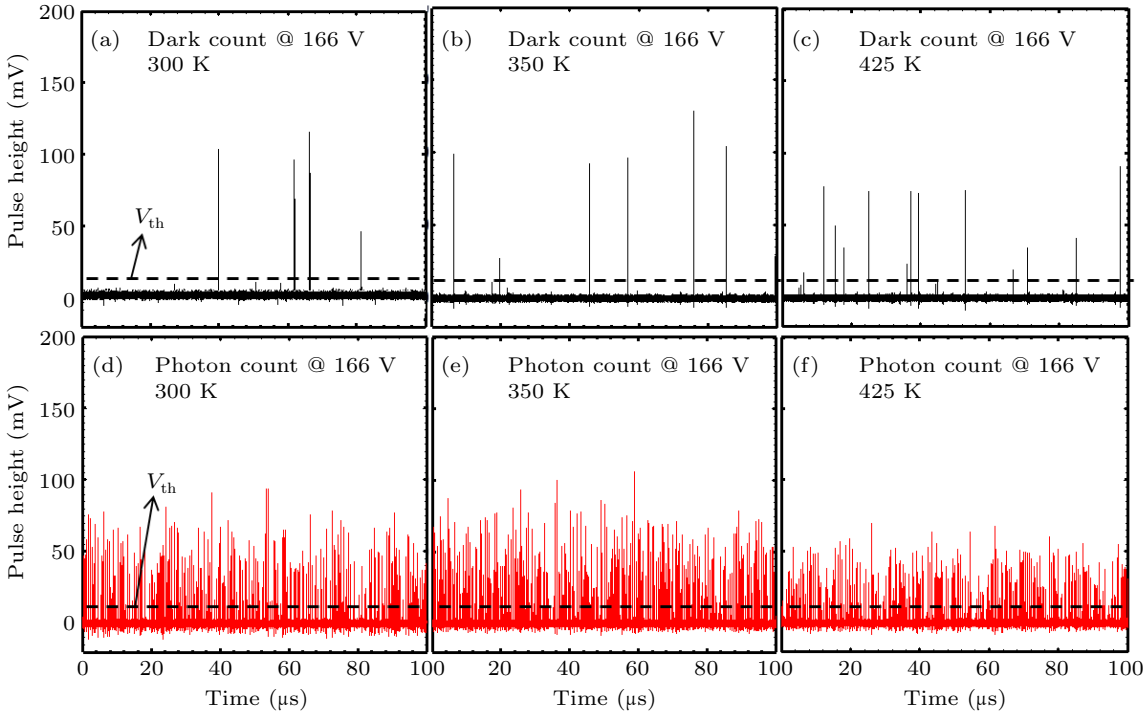


Fig. 6. Single-photon counting measurements at different temperatures: dark and photon count spectra with a fixed bias voltage of 166 V in Geiger mode.

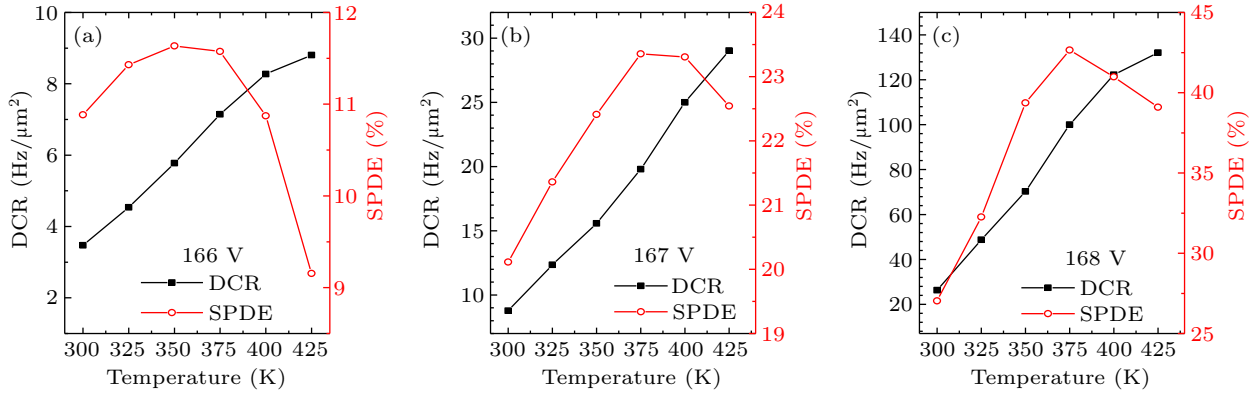


Fig. 7. Dependence of DCR and SPDE on the temperature at different bias voltages for 4H-SiC APDs.

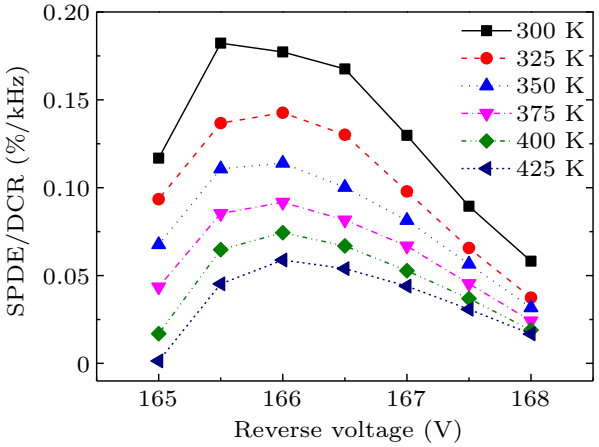


Fig. 8. The ratio of SPDE to DCR as a function of reverse voltage of 4H-SiC APDs at different temperatures.

The ratio of SPDE to DCR as a function of the reverse bias voltage of 4H-SiC APDs at various temperatures is plotted in Fig. 8. The ratio of SPDE to DCR represents the signal to noise ratio of APD devices. It can be seen from Fig. 8 that the SPDE/DCR ratio is reduced as the temperature increases at a given bias voltage, since the DCR increases quickly at higher temperatures. Furthermore, the SPDE/DCR ratio increases first then decreases as the reverse voltage increases at a given temperature. This is because although both of DCR and SPDE increase with the reverse bias voltage (see Fig. 7), the increase in DCR becomes larger than that of SPDE, and consequently the SPDE/DCR ratio declines at higher voltages. Therefore, in practical applications, it is necessary to optimize the bias voltage of 4H-SiC APDs carefully for a higher SPDE/DCR ratio.

4. Conclusion

The high-temperature performance of 4H-SiC APDs in both linear and Geiger modes was extensively investigated at a fixed bias voltage for practical applications. It is proved that the fabricated 4H-SiC APDs can operate very stably and

reliably at high temperatures. In linear mode, the dark current at 95% of breakdown voltage increases slightly but remains lower than 40 pA as the temperature increases from 300 K to 425 K, and a very small temperature coefficient of < 8 mV·K^{-1} is obtained for the avalanche breakdown voltage. In Geiger mode, the fabricated 4H-SiC APDs can be self-quenched without a large quenching resistor in a passive quenching circuit. Non-monotonic variation of the SPDE as a function of temperature with a fixed bias voltage is observed and analyzed for the first time. The results in this work can provide a fundamental reference for researchers in the field of 4H-SiC APD UV detectors.

Acknowledgments

Project supported by the National Natural Science Foundation of China (Grant No. 61974134) and Hebei Province Outstanding Youth Fund (Grant No. F2021516001).

References

[1] Xin X, Yan F, Sun X, *et al.* 2005 *Electron Lett.* **41** 212
[2] Guo X, Beck A L, Li X, *et al.* 2005 *IEEE J. Quantum Electron.* **41** 562
[3] Guo X, Rowland L B, Dunne G T, *et al.* 2006 *IEEE Photon. Technol. Lett.* **18** 136
[4] Liu H D, Guo X, McIntosh D, *et al.* 2006 *IEEE Photon. Technol. Lett.* **18** 2508
[5] Hu J, Xin X, Li X, *et al.* 2008 *IEEE Trans. Electron Devices* **55** 1977
[6] Liu H D, McIntosh D, Bai X, *et al.* 2008 *IEEE Photon. Technol. Lett.* **20** 1551
[7] Liu H D, Zheng X, Zhou Q, *et al.* 2009 *IEEE J. Quantum Electron.* **45** 1524
[8] Vert A, Soloviev S, Fronheiser J, *et al.* 2008 *IEEE Photon. Technol. Lett.* **20** 1587
[9] Zhou Q, Liu H D, McIntosh D C, *et al.* 2009 *IEEE Photon. Technol. Lett.* **21** 1734
[10] Bai X, Liu H D, McIntosh D C, *et al.* 2009 *IEEE J. Quantum Electron.* **45** 300
[11] Zhou Q, McIntosh D, Liu H D, *et al.* 2011 *IEEE Photon. Technol. Lett.* **23** 299
[12] Hu J, Xin X, Zhao J H, *et al.* 2011 *IEEE Trans. Nucl. Sci.* **58** 3343
[13] Zhou X, Tan X, Wang Y G, *et al.* 2019 *Chin. Opt. Lett.* **17** 090401
[14] Cai X, Zhou D, Yang S, *et al.* 2016 *IEEE Photon. J.* **8** 6805107
[15] Zhou X, Han T, Lv Y, *et al.* 2018 *IEEE Electron Device Lett.* **39** 1724
[16] Zhou X, Li J, Lu W, *et al.* 2018 *Chin. Opt. Lett.* **16** 060401
[17] Liu F, Yang S, Zhou D, *et al.* 2015 *Chin. Phys. Lett.* **32** 88503
[18] Liu F, Zhou D, Lu H, *et al.* 2015 *Chin. Phys. Lett.* **32** 128501
[19] Vert A, Soloviev S, Bolotnikov A, *et al.* 2009 *IEEE Sensors Conference*
[20] Zhou X, Tan X, Lv Y, *et al.* 2019 *IEEE Electron Dev. Lett.* **40** 1591
[21] Yan F, Qin C, Zhao J H, *et al.* 2003 *Solid-State Electronics* **47** 241
[22] Li L, Zhou D, Lu H, *et al.* 2017 *IEEE Photon. J.* **9** 6804207
[23] Zhou X, Tan X, Lv Y, *et al.* 2020 *Opt. Express* **28** 29245
[24] Guo X, Beck A L, Huang Z, *et al.* 2006 *IEEE Trans. Electron Devices* **53** 2259
[25] Cha H Y, Soloviev S, Zelakiewicz S, *et al.* 2008 *Sensors J.* **8** 233
[26] Zhou D, Liu F, Lu H, *et al.* 2014 *IEEE Photon. Technol. Lett.* **26** 1136
[27] Yang S, Zhou D, Cai X, *et al.* 2017 *IEEE Trans. Electron Devices* **64** 4532
[28] Raghunathan R, Baliga B J, *et al.* 1999 *Solid-State Electronics* **43** 199